Polymer 50 (2009) 1533–1540

Contents lists available at ScienceDirect

Polymer

journal homepage: www.elsevier.com/locate/polymer

Investigation of water diffusion in poly(3-hydroxybutyrate-*co*-3-hydroxyhexanoate) by generalized two-dimensional correlation ATR–FTIR spectroscopy

Hua-Xiao Yang, Min Sun, Ping Zhou*

The Key Laboratory of Molecular Engineering of Polymers, Ministry of Education, Department of Macromolecular Science, Fudan University, 220 Handan Road, Shanghai 200433, PR China

ARTICLE INFO

Article history:
Received 2 October 2008
Received in revised form
28 November 2008
Accepted 17 January 2009
Available online 24 January 2009

Keywords:
Poly(3-hydroxybutyrate-*co*-3-hydroxyhexanoate), PHBHHx
Water diffusion
2D correlation

ABSTRACT

Water diffusion process in biodegradable poly(3-hydroxybutyrate-*co*-3-hydroxyhexanoate) (PHBHHx, HHx = 12 mol%) was investigated by generalized 2D correlation time-resolved ATR–FTIR spectroscopy based on the analysis of ν(OH) stretching and δ(OH) bending bands of water as well as ν(C=O) and ν(C–O–C) stretching bands of PHBHHx. Three states of water were figured out during water diffusion process. They are bulk water, bound water and free water. The water diffusion mechanism was suggested as: water molecules firstly diffuse into the micro-voids in bulk water form or are dispersed on the surface in free water form, and then penetrate into the polymer matrix in hydrogen bound water with the hydrophilic groups of PHBHHx. Moreover, water molecules diffuse into the loose amorphous phase and then into compact crystalline phase. Water diffusion coefficient in PHBHHx was thus evaluated as $7.8 \pm 0.7 \times 10^{-8}$ cm^2 s^{-1} for the PHBHHx with crystallinity of 16.2 ± 0.3% at 293 K.

1. Introduction

Poly(3-hydroxybutyrate-*co*-3-hydroxyhexanoate) (PHBHHx, HHx = 12 mol%) is a microorganism synthesized degradable polyester, one of the polyhydroxyalkanoate (PHA) family [1,2] which includes polyhydroxybutyrate (PHB) [3], poly-3-hydroxybutyrate-*co*-poly-3-hydroxyvalerate (PHBV) [4,5], PHBHHx with different HHx molar percentages [6] and so on. During the past decade, PHAs have attracted more and more attentions for their microorganism synthesis [3,7], biodegradable and biocompatible properties [8,9]. One of the simplest and substantively manufactured PHAs polymers is PHB, which was demonstrated potential in the tissue engineering utilization [10]. Recently, the TephaFLEX® absorbable suture made of poly(R-4-hydroxybutyrate) has been approved by the US Food and Drug Administration (FDA) for clinical applications [11]. But the high crystallinity degree of PHB [12] limits its further and wider applications in some extent, especially when some critical properties, such as outstanding elasticity and elongation at break, are required. Several methods have been proposed to reduce its crystalline degree by breaking the ordered crystalline region to improve the elasticity of PHB, such as blending with the flexible poly(vinyl alcohol) (PVA) [13], PLLA (poly(L-lactic acid)) [14,15] or oligoester [16], or synthesizing the co-polymers like PHBHHx [3] and PHBV [5,17] by regulating feeding recipes to the microorganism. Among these methods, synthesizing the co-polymer has been proved to be one of the most effective methods for a better and broader application of PHB as the tissue engineering materials. Alata et al. [6] and Zhao et al.[1] reported that PHBHHx (HHx = 12 mol%) had the elongation at break of ~500% and maintained applicable tensile strength of ~20 Mpa, while PHB film had the elongation at break of <10% and tensile strength of ~30 Mpa. Ozaki et al. [18–22] utilized wide-angle X-ray diffraction (WAXD), differential scanning calorimeter (DSC), infrared spectroscopy (IR) and generalized two-dimensional correlation FTIR spectroscopy to investigate the detailed crystalline and amorphous characters and thermal behaviors during melting and cooling processes of the PHBHHx (HHx varied from 2.5 to 12 mol%). They found an intermolecular interaction (hydrogen bonding) between the C=O group in one helical structure and the CH_3 group in the other helical structure during melting and crystallization processes of PHBHHx and PHB matrix. Interestingly, the investigations [23] showed that the physical property of PHBHHx could effect the change in the phenotype of SMCs (smooth muscle cells) *in vitro*. More flexible scaffold or film could help SMCs maintained or induced into the contractile phenotype which is a mature cell type in adult vessels, that is to say, the scaffold not only played as a supporter for the cell and tissue growth but its physical properties, such as crystalline degree, interaction with water, could also

* Corresponding author. Tel.: +86 21 55664038; fax: +86 21 65640293.
E-mail address: pingzhou@fudan.edu.cn (P. Zhou).

0032-3861/$ – see front matter © 2009 Elsevier Ltd. All rights reserved.
doi:10.1016/j.polymer.2009.01.038

modulate the proliferation, differentiation, migration of certain cells.

Generally, when the polymer material is used to construct a scaffold and implanted into the body, one of the most important things one needs to concern is the nutrition transportation within cell and scaffold. The water diffusion ability in the scaffold plays a key role in this process. Water diffusion process is affected by many factors, such as polymer categories, ambient humidity, and polymer crystalline degree and so on. Among these factors, the crystallinity of the polymer is one of the most important factors. Perrin et al. [24] indicated that the higher the crystallinity of the poly(vinyl alcohol) (PVA) membrane, the smaller the diffusion coefficient. Miguel and Iruin [25] compared the water diffusion coefficients between PHB and PHBV films at 40 °C, and found that the PHBV film with a lower crystallinity than PHB [2] showed higher water diffusion coefficient than PHB film. Sammon et al. [26,27] also found the similar result of the water diffusion in PET (polyethylene terephthalate) film. These results are may be understandable because the water diffusing process in high crystallinity of polymer film could be blocked in some extent. As a result, the fundamental study of PHBHHx physical properties including crystallinity and water diffusion ability becomes necessary for the further medical applications of PHBHHx. In addition, water diffusion and sorption in polymer materials have also great effects on other applications, for example, the packaging industry [28], separation of gas, liquid or vapor mixtures in membrane process [29], fuel cell [30] and drug delivery [31].

Among the methods of measuring water diffusion process in polymer matrix, ATR–FTIR is one of the most effective ways to detect the whole diffusion process in real time [32]. The *in situ* time-resolved ATR–FTIR can measure not only the water diffusion coefficient [33] but also the molecular interaction between water and polymer [34]. Sammon [26,35,36] investigated the water diffusion process and found four different states of water OH stretching vibration in polymer matrices, like PET and PVC (polyvinyl chloride) using ATR–FTIR spectroscopy. With the same method, Peng and his colleagues [37,38] proposed the water diffusion process in poly(ε-caprolactone) (PCL) polymer matrix as: water molecules diffused firstly into the free voids of PCL matrix or were molecularly dispersed into the matrix and then formed the hydrogen bonds with hydrophilic C═O group of PCL forming the bound water in polymer matrix. In addition, Iordanskii [39–41] studied the water diffusion and sorption in the PHB films by the microgravimetry method and obtained the water diffusion coefficient of 1.5×10^{-8} cm^2 s^{-1} at 313 K. Although the water diffusion processes in some polymers were investigated, the results in the PHBHHx material have not been reported yet.

Generalized two-dimensional (2D) correlation spectroscopy primarily proposed by Noda et al. [42] in 1993 is a generally applicable mathematical formalism which can construct a 2D correlation spectroscopy from numerous transient or time-resolved variations of spectra having an arbitrary waveform. The 2D correlation spectroscopy responses any variations in the form of autocorrelation peaks and cross-peaks to the fluctuations, such as time, temperature, pressure, electric field strength and concentration, etc. It can provide the information of different molecular functionalities as well as the relative sequence order of the spectral intensity changes taking place under the course of the perturbation for the revealing of molecular dynamics in a polymer in molecular scale [42]. In addition, the 2D correlation spectroscopy can be also used to help the assignment of the spectral bands [18,20,43,44].

In this work, we studied the molecular interaction between water and PHBHHx matrix during water diffusing process. Based on the analysis of the interesting bands in 1D and 2D FTIR spectrum as well as the molecular crystallinity, we attempted to reveal the water roles and evaluate the water diffusion coefficient in PHBHHx. The results would be useful for better understanding of the mechanism of water diffusion in the PHBHHx matrix, which is significant for the material to be efficiently utilized in the medicine, packaging and agriculture fields.

2. Materials and experimental

2.1. Materials

PHBHHx powder (molecular weight = 100,000, HHx = 12 mol%) was kindly donated by Prof. Guo-Qiang Chen in Tsinghua University. It was purified by dissolving it in the dichloromethane (CH_2Cl_2) solution, and fully refluxed at 40 °C for half an hour, and then filtered through qualitative filter paper, and re-precipitated in *n*-hexane solution. The resultant solid sample was dried at room temperature for more than 24 h, and stored in the desiccator for later use. About 0.3 g purified PHBHHx powder was dissolved in 10 mL CH_2Cl_2, and then the transparent solution was cast on a glass plate in diameter of 60 mm in fume hood at room temperature for 24 h. A film of thickness 97 ± 1 μm was obtained.

2.2. Crystalline degree of pure PHBHHx film

The crystalline degree of the pure PHBHHx film was measured by differential scanning calorimetry (DSC, Pyris 1, PerkinElmer Thermal Analysis). The sample (7.2 mg) was heated from 20 to 160 °C at a rate of 10 °C/min. The melting temperature (T_m) and fusion enthalpy (ΔH_m) were determined by the endotherms in DSC. The PHBHHx crystalline degree (C%) was calculated based on the method as following Eq. (1) [23,45].

$$C_{\mathrm{PHBHHx}}\% = \Delta H_{\mathrm{m(PHBHHx)}} / \Delta H^0_{\mathrm{m(PHB)}} \times 100\% \quad (1)$$

In Eq. (1), $\Delta H^0{}_{\mathrm{m(PHB)}}$, 146.6 J/g, is the enthalpy of melting per gram of PHB in 100% crystalline degree [23,45], and $\Delta H_{\mathrm{m(PHBHHx)}}$ is an apparent melting enthalpy of PHBHHx measured here. We took the PHBHHx with HHx = 0% as a pure PHB. HHx was thought being in a pure amorphous motif in the PHBHHx [6,12,20]. Therefore, the crystalline degree of PHB domain determined that of PHBHHx. Four samples were measured and an average crystalline degree and standard deviation of $C_{\mathrm{PHBHHx}} \pm$ SD% were determined by four results.

2.3. Water diffusion detected by time-resolved ATR–FTIR spectroscopy

All the time-resolved infrared spectra were recorded at 26 °C by FTIR spectrometer (Nicolet Nexus Smart ARK) equipped with a DTGS detector, a horizontal ATR cell and a zinc selenide trapezoidal IRE ATR crystal (refractive index of 2.4). The detailed experimental process was referred to the literature [38]. In brief, a PHBHHx film with size of 2 (width) × 4 (length) × 0.00974 (thickness) cm was covered on the IRE crystal, and then a same size of pre-wetted filter paper by 0.1 ml water was mounted on the surface of the PHBHHx film. Once the wet filter paper contacted with the film, the FTIR spectrum was recorded using a macro program. A series of time-resolved spectra were collected at a resolution of 4 cm^{-1} with 16 scans. The interval between two adjacent spectra was 20 s. The spectral range was 4000–650 cm^{-1}. All the original spectra were baseline corrected using OMNIC 6.1a.

Fieldson and Barbari [46] put forward a diffusion equation (Eq. (2)) especially useful for the estimation of the molecule diffusion coefficient base on the IR data. The equation was deduced from the Fickian diffusion of a single solute in polymer film.

$$\frac{A_t}{A_{eq}} = 1 - \frac{8\gamma}{\pi[1-\exp(-2\gamma L)]} \times \sum_{n=0}^{\infty}\left[\frac{\exp(g)[f\exp(-2\gamma L)+(-1)^n(2\gamma)]}{(2n+1)\left(4\gamma^2+f^2\right)}\right] \quad (2)$$

$$\gamma = \frac{-D(2n+1)^2\pi^2 t}{4L^2} \quad (3)$$

$$f = \frac{(2n+1)\pi}{2L} \quad (4)$$

where A_t is the integrated IR absorbance of a functional group associated with the diffusion process at time t, and A_{eq} is an equilibrium value. γ is the reciprocal of the penetration depth of the evanescent wave, L is the thickness of the polymer film, and D is the diffusion coefficient which is the only changeable parameter in this equation. The water diffusion coefficient in PHBHHx film can be obtained through the non-linear curve fitting [33] according to Eq. (2) on the basis of intensity variation of the water ν(OH) stretching and δ(OH) bending bands *versus* time herein.

2.4. 2D correlation analysis

Generalized 2D correlation spectroscopy is based on the perturbation of samples with time, temperature, concentration, reaction time and so on.

The perturbation-induced changes in spectral intensities $y(\nu, t)$ can be obtained as a function of a exterior perturbation variable t, where the data are collected as t change from T_{min} to T_{max}. Here t can be any reasonable physical variable, such as water diffusion time as used in this work. The perturbation-based spectral profile $\tilde{y}(\nu, t)$ is expressed by

$$\tilde{y}(\nu,t) = \begin{cases} y(\nu,t)-\overline{y}(\nu) & \text{for } T_{min} \le t \le T_{max} \\ 0 & \text{otherwise} \end{cases} \quad (5)$$

where $\overline{y}(\nu)$ is an average of the trace profiles obtained over the observed perturbation range and used as a reference spectrum:

$$\overline{y}(\nu) = \frac{1}{T_{max}-T_{min}}\int_{T_{min}}^{T_{max}} y(\nu,t)\mathrm{d}t \quad (6)$$

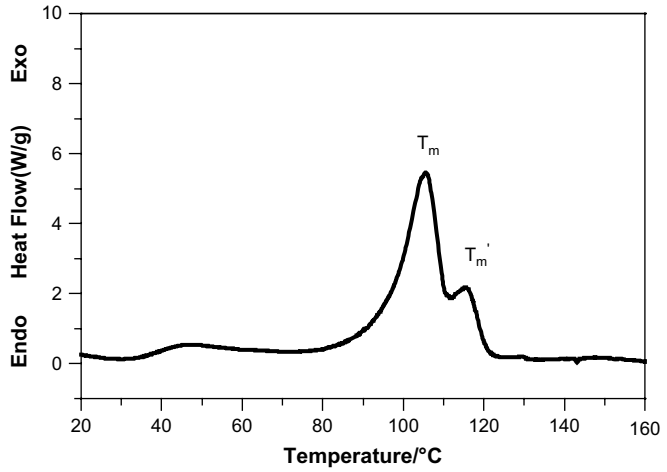

Fig. 1. DSC curve of the pure PHBHHx (HHx = 12 mol%) film at a heating rate of 10 °C/min in the temperature range of 20–160 °C. T_m and T_m' represent the melting peaks of two types lamellae in crystal.

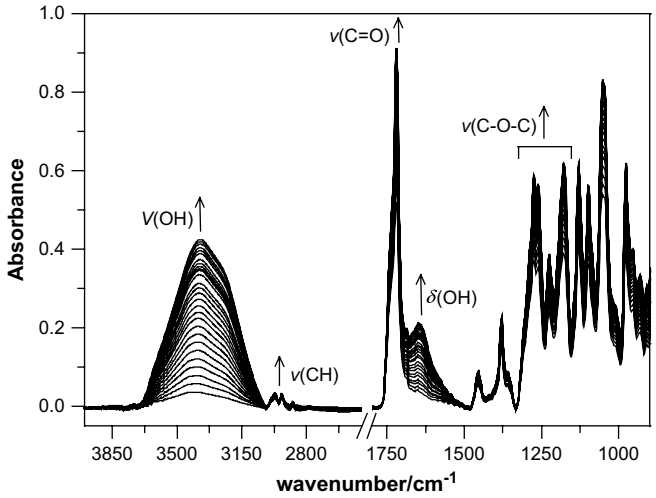

Fig. 2. ATR–FTIR spectra of PHBHHx (HHx = 12 mol%) as water diffusion. The arrows indicate the directions of intensity changes during diffusion process.

The generalized 2D correlation function for the perturbation-based spectra is defined as [42,43]:

$$\Phi(\nu_1,\nu_2)+i\Psi(\nu_1,\nu_2) = \frac{1}{\pi(T_{max}-T_{min})}\int_0^{\infty}\tilde{z}_1(\nu_1,\omega)\tilde{z}_2^*(\nu_2,\omega)\mathrm{d}\omega \quad (7)$$

where $\Phi(\nu_1,\nu_2)$ and $\Psi(\nu_1,\nu_2)$ are called, respectively, generalized synchronous and asynchronous 2D correlation spectrum. $\tilde{z}_1(\nu_1,\omega)$ is the Fourier transformation of the data $\tilde{y}_1(\nu_1,t)$, and $\tilde{z}_2^*(\nu_2,\omega)$ is the corresponding Fourier conjugate of the data $\tilde{y}_2(\nu_2,t)$.

In the generalized 2D correlation spectrum, a cross-peak (ν_1,ν_2) found in a synchronous 2D correlation spectrum $\Phi(\nu_1,\nu_2)$ represents the simultaneous or coincidental changes in spectral intensities at corresponding variables ν_1 and ν_2, as an external perturbation is applied. The sign of a synchronous cross-peak becomes positive if the response at ν_1 is in the same direction as that at ν_2, either increasing or decreasing simultaneously, as the external physical variable (e.g. diffusion time) is changed. In contrast, a negative cross-peak indicates that the response at ν_1 is in the opposite direction to that at ν_2. A cross-peak present in an asynchronous 2D

Table 1
Band assignments for the ATR-FTIR spectra of water and PHBHHx polymer film.

Wave number (cm^{-1})	Assignment	References
3700–3000	OH stretching band region of water	
3675	Free water	
3648, 3438	Bound water associated with polymer matrix	[33,37,38]
3234	Bulk water in polymer matrix	
1800–1700	C=O stretching band region of PHBHHx	
1740	Crystalline phase	
1735	Semi-crystalline phase	[12,18,20]
1718	Amorphous phase	
1700–1550	OH bending band region of water	
1662	Bulk water in polymer matrix	
1625, 1637	Bound water associated with polymer matrix	[33,49,52]
1583	Free water	
1300–1150	C–O–C stretching band region of PHBHHx	
1272, 1224, 1209	Crystalline phase	[20,21]
1245, 1209, 1176	Amorphous phase	

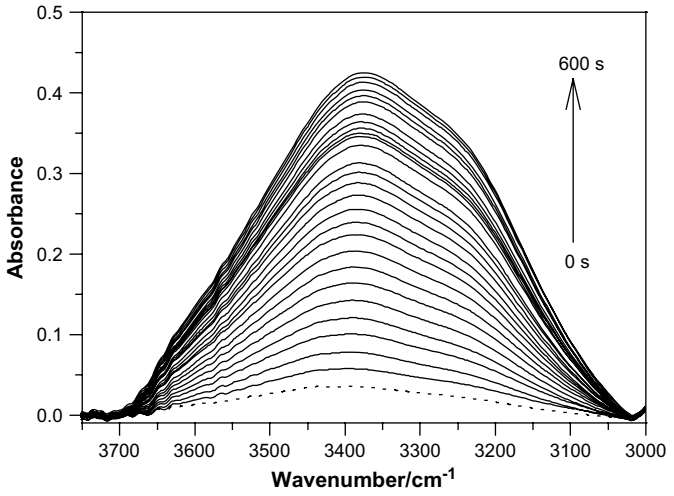

Fig. 3. FTIR spectra of the water ν(OH) stretching band in PHBHHx (HHx = 12 mol%) film within the region of 3700–3000 cm^{-1}. The short dot line represents the starting spectrum, and the spectral interval is 20 s.

correlation spectrum $\Psi(\nu_1,\nu_2)$ indicates that the responses at corresponding variables ν_1 and ν_2 vary out of phase with each other as the perturbation is applied. The response at ν_1 occurs earlier than that at ν_2 if the signs of the cross-peaks (ν_1,ν_2) in both synchronous and asynchronous spectra are the same; in contrast, the response at ν_1 occurs later than that at ν_2 if the signs are different.

2D correlation analysis was performed by using the 2D-shige 1.3 software composed by Shigeaki Morita (Kwansei-Gakuin University, Japan). All the spectra measured previously were baseline corrected prior to the 2D correlation analysis. The shaded and unshaded areas in the 2D correlation contour maps denoted the negative correlation peaks and positive correlation peaks, respectively.

3. Results and discussion

3.1. Crystalline degree of pure PHBHHx film

DSC curve of the pure PHBHHx film was shown in Fig. 1, which shows two melting temperatures of T_m at 104.8 ± 0.4 °C and T_m' at 115 °C that are consistent to the literature reports [22,47,48]. Two melting peaks may be resulted from two types of lamellae in crystal [22]. The fusion enthalpy ($\Delta H_{m(PHBHHx)}$) of 23.8 ± 0.4 J/g is obtained by the integration of the two peaks. According to Eq. (1), the crystalline degree of pure PHBHHx film was calculated to be 16.2 ± 0.3%.

3.2. Changes in the ν(OH) stretching band

Fig. 2 is the ATR–FTIR spectrum of PHBHHx film as water diffused. The assignments of the peaks were summarized in Table 1. To study the molecular interaction between water and polymer during the water diffusion in the PHBHHx films, we mainly observed the changes in ν(OH) stretching band of 3700–3000 cm^{-1} and δ(OH) bending band of 1700–1550 cm^{-1} in water, ν(C=O) stretching band of 1800–1700 cm^{-1} and ν(C–O–C) stretching band of 1300–1160 cm^{-1} in PHBHHx.

Fig. 3 shows the increased absorbance of water ν(OH) stretching bands at about 3400 cm^{-1} and 3200 cm^{-1} during water diffusion in the PHBHHx film. The 2D correlation FTIR spectra shown in Fig. 4 provide further information of water states in the PHBHHx film. There are two autocorrelation peaks along the diagonal in the synchronous spectrum (Fig. 4A), which locate at 3234, 3234 cm^{-1} and 3438, 3438 cm^{-1}. These two autocorrelation peaks are assigned to the water ν(OH) stretching bands [37,38]. Besides, three positive cross-peaks at 3234, 3438 and 3438, 3648 and 3438, 3675 cm^{-1} are shown in the upper triangle zone of the contour map of asynchronous spectrum (Fig. 4B), which indicate that there are four different components corresponding to 3234, 3438, 3648, 3675 cm^{-1} interacting with each other during water diffusion. Sammon et al. summarized that there were four states of water existing in several categories of polymer matrix, that is, bulk water forming strong hydrogen bonds between each water molecule, strong bound water interacting with hydrophilic groups, like C=O, −OH etc., in polymer matrices, weak bound water interacting with hydrophobic groups like CH_2&CH_3 in polymer matrices and free water not interacting with other molecules [27,35]. Accordingly, herein, 3234 cm^{-1} is assigned to the bulk water in polymer matrix, 3438 and 3648 cm^{-1} are assigned to the form of bound water with polymer by hydrogen bonds, and the band at 3675 cm^{-1} is attributed to the form of free water accordingly. Additionally, based on Noda's rule [42], the positive cross-peaks in 3234, 3438, and 3438,

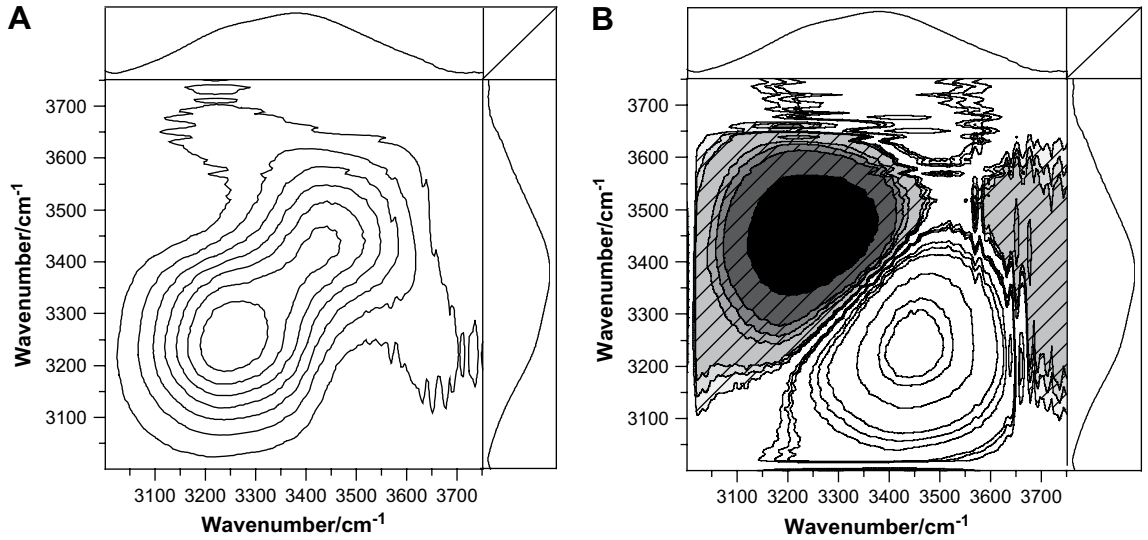

Fig. 4. Generalized 2D correlation FTIR spectra of water ν(OH) stretching band of water in the region of 3700–3000 cm^{-1}. (A) and (B) are synchronous and asynchronous contour maps, respectively. The shaded and unshaded areas represent negative and positive correlation peaks, respectively.

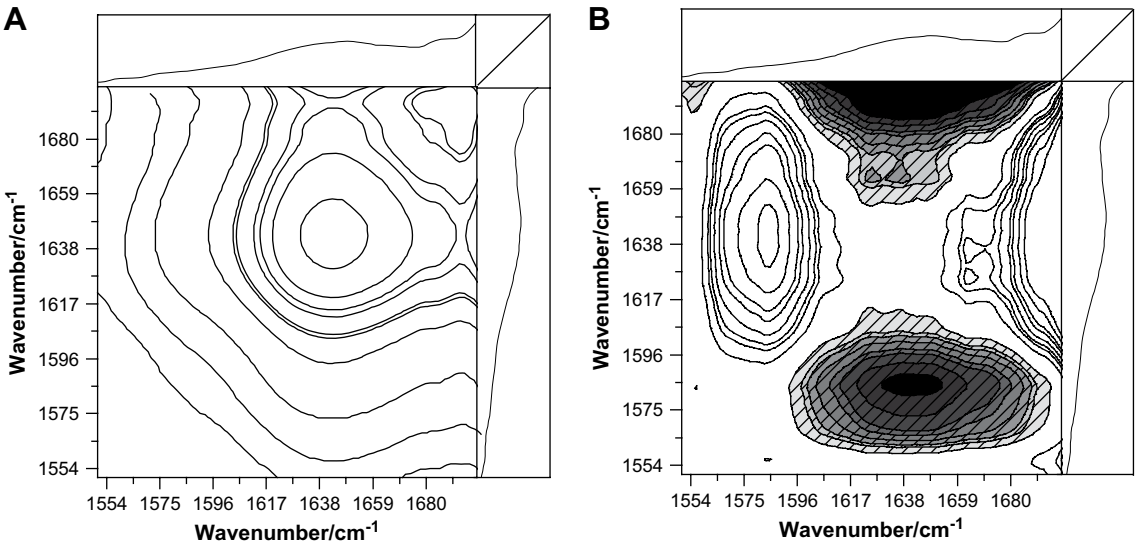

Fig. 5. Generalized 2D correlation FTIR spectra of water δ(OH) bending band of water in the region of 1700–1550 cm^{-1}. (A) and (B) are synchronous and asynchronous contour maps, respectively. The shaded and unshaded areas represent negative and positive correlation peaks, respectively.

3648 cm^{-1} in synchronous (Fig. 4A) and asynchronous spectra (Fig. 4B) indicate that the peak of 3234 cm^{-1} varies prior to the peaks of 3438 cm^{-1}, the peak of 3438 cm^{-1} varies prior to the peaks of 3648 cm^{-1}. Thus, these three bands vary in the sequence order as: 3234 → 3438 → 3648 cm^{-1}, therefore the water molecules diffuse into the PHBHHx film in bulk form firstly present in the micro-voids formed when PHBHHx film was cast, and then in strong hydrogen bonded form interacting with the hydrophilic groups like C═O [37,38] in the PHBHHx.

3.3. Changes in δ(OH) bending band

When more water molecules diffuse into PHBHHx film, the intensity of the δ(OH) bending band around 1648 cm^{-1} increases gradually as demonstrated in Fig. 2. Moreover, 2D synchronous correlation spectrum shows that, a strong positive cross-peak and two weak positive cross-peaks are developed at 1625, 1662 and 1637, 1662 and 1583, 1645 cm^{-1} respectively (Fig. 5A). Correspondingly, two weak negative cross-peaks at 1625, 1662, 1637, 1662 cm^{-1} and a moderate positive cross-peak at 1583, 1645 cm^{-1} were generated in asynchronous spectrum (Fig. 5B). According to Noda's rule [42], the change in intensity at 1662 cm^{-1} varies earlier than the changes in intensities at 1625, 1637 cm^{-1}, and the change in intensity at 1583 cm^{-1} is prior to the change in intensity at 1625 cm^{-1}. In brief, the change sequence order is 1662 → 1625, 1637 cm^{-1} and 1583 →1645 cm^{-1}. Peng et al. assigned three states of water in PP (polypropylene) film during water diffusion as that [49]: the 1662 cm^{-1} to the aggregated water in bulk water form; the 1645 cm^{-1} to the aggregated water with moderate hydrogen bond (partially bonded with polymer matrix); and the 1592 cm^{-1} to the free water. In our results, the band at 1662 cm^{-1} could be assigned to be bulk water, 1625 and 1637 cm^{-1} assigned to the strong bound water in polymer matrix with C═O and C–O–C groups and 1583 cm^{-1} assigned to the even dispersed free water. Based on the change in sequence order of these bands, the water diffusion mechanism in PHBHHx film could be proposed as: water molecules diffuse into the micro-voids in bulk water form (at 1662 cm^{-1}) or are dispersed on the surface of film in free water (at 1583 cm^{-1}), and then penetrate into the film matrix in hydrogen bonded form with the hydrophilic groups C═O and C–O–C of polymer (demonstrated at 1625 and 1637 cm^{-1}).

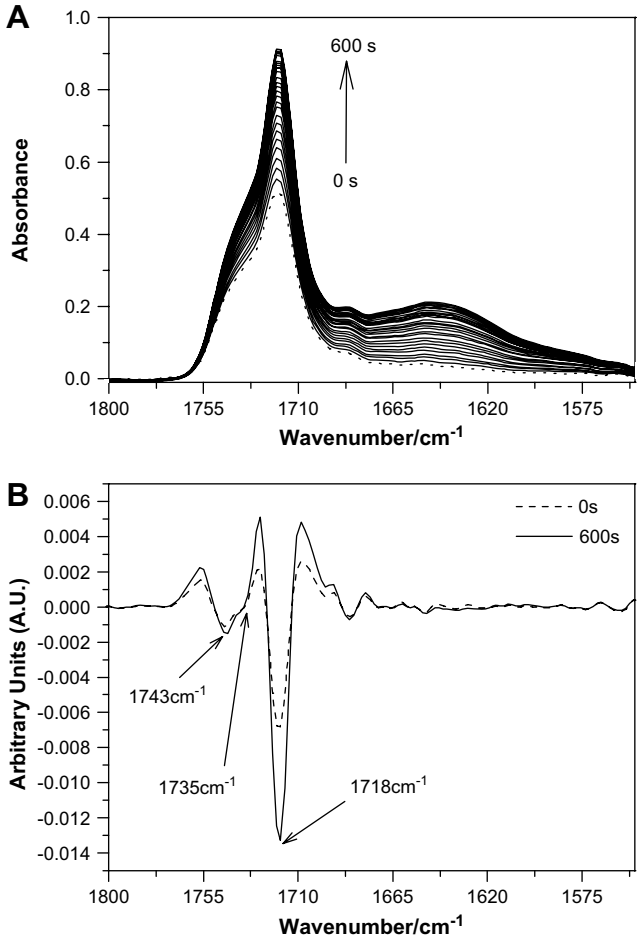

Fig. 6. (A) FTIR spectra of the ν(C═O) stretching band (1800–1700 cm^{-1}) and the δ(OH) bending band (1700–1600 cm^{-1}) during water diffusion in the region of 1800–1500 cm^{-1}. The short dot line represents the starting spectrum, and the spectral interval time is 20 s. (B) Secondary derivative of two of FTIR spectra in (a). The short dot line represents the starting point of water diffusion in film, and the solid line represents the ending point (600 s) of water diffusion in film.

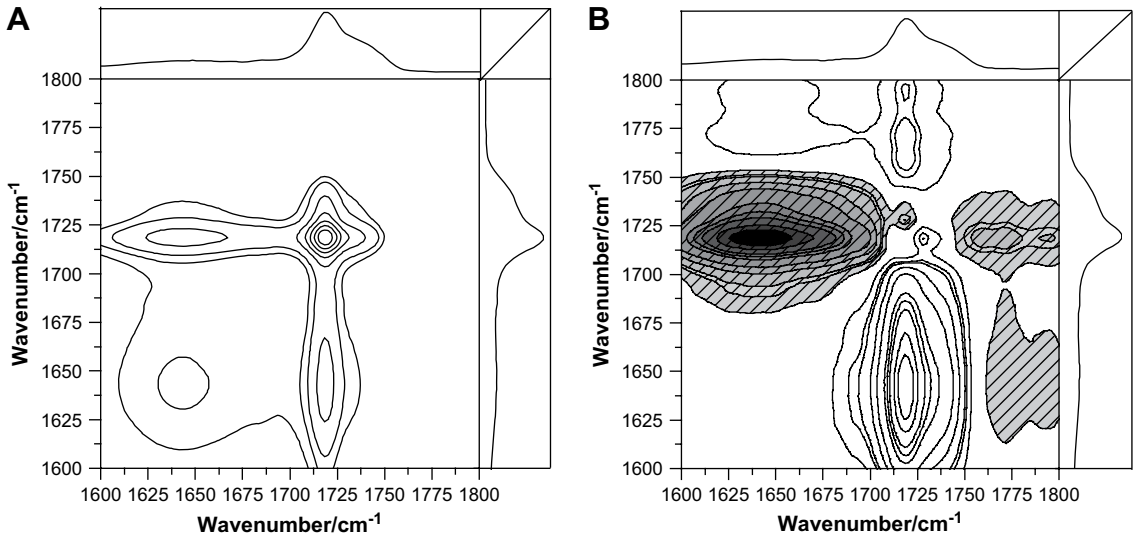

Fig. 7. Generalized 2D correlation FTIR spectra of ν(C=O) stretching band of PHBHHx (HHx = 12 mol%) at the region of 1800–1600 cm^{-1}. (A) and (B) are synchronous and asynchronous contour maps, respectively. The shaded and unshaded areas represent negative and positive correlation peaks, respectively.

3.4. Changes in ν(C=O) stretching band

Fig. 6A shows the FTIR spectra of ν(C=O) stretching band during water diffusion in the PHBHHx. It is found that the intensities of a sharp band at 1718 cm^{-1} and a broad shoulder band at 1740 cm^{-1} increase gradually during water molecules penetrating into the polymer film, demonstrating that the hydrophilic group C=O in PHBHHx associated with water during water diffusion. Padermshoke et al. investigated the melting process of PHBHHx bulk by FTIR and generalized 2D correlation spectroscopy [12,20,22]. They found that the intensity of sharp band at 1720 cm^{-1} decreased gradually during the PHBHHx bulk melting, while the intensity of broad-band at 1740 cm^{-1} increased. Authors assigned 1720 cm^{-1} to the crystalline phase and 1740 cm^{-1} to the amorphous phase, based on the fact that the crystalline phase was destroyed and transformed to the amorphous phase step by step during the melting process in a semi-crystalline polymer. In addition, they also found a peak near 1730 cm^{-1}, and assigned it to a semi-crystalline phase when the starting point of heating was around 30 °C. In the present work, when the starting and ending FTIR spectral curves in Fig. 6a were secondly differenced, the peak around 1735 cm^{-1} was also found in Fig. 6B.

Furthermore, we constructed the generalized 2D correlation FTIR spectrum within region of 1800–1600 cm^{-1} to view insight into the water diffusing process. Fig. 7A and B show the synchronous and asynchronous contour maps, respectively. The positive cross-peak at 1645, 1718 cm^{-1} in the synchronous contour map (Fig. 7A) indicates that the water ν(OH) bending band at 1645 cm^{-1} varies in the same direction with the PHBHHx ν(C=O) band at 1718 cm^{-1}. It demonstrates the interaction, e.g. hydrogen bonding, presents between water and PHBHHx and increases during the water diffusion. The positive cross-peak at 1718, 1729 cm^{-1} in synchronous contour map (Fig. 7A) and the negative same cross-peak in asynchronous contour map (Fig. 7B) indicate the interaction existing between two bands at 1718 and 1729 cm^{-1}. Based on Noda's rule [42], the change of intensity of 1729 cm^{-1} is prior to the change of 1718 cm^{-1}. Consequently, it may indicate that water molecules diffuse into the low crystalline degree phase (1729 cm^{-1}) firstly, and then into the high crystalline degree phase (1718 cm^{-1}). In other words, it is more convenient and efficient for the water molecules to diffuse in the loose amorphous phase than in the compact crystalline phase of PHBHHx film. The crystalline degree of 16.2 ± 0.3% of the PHBHHx herein is much lower than that of 60 ± 5% of PHB [3,45]. Therefore, we thought that water molecules more favorably penetrate through the PHBHHx than through the PHB matrix.

3.5. Changes in ν(C–O–C) stretching band

Fig. 8 shows the spectra of PHBHHx between 1300 and 1160 cm^{-1} during water diffusion. There are five dominant peaks at 1290, 1274, 1261, 1226 and 1176 cm^{-1} in Fig. 8, which were slight red-shifted from 1289, 1278, 1264, 1228 and 1182 cm^{-1} observed by Sato and Padermshoke et al. [20,22], demonstrating the interaction of hydrogen bonding between water molecules and C–O–C groups. Sato et al. [20,22] investigated the melting process of PHBHHx (HHx = 2.5, 3.4 and 12 mol%) from 30 to 140 °C measured by 1D and 2D FTIR in the range from 1300 to 1150 cm^{-1} which is multi-peak combination of ν(C–O–C) stretching vibration and δ(CH) and $\delta(CH_2)$ bending vibrations [22]. Sato et al. found the intensities of bands at 1289, 1278, 1264 and 1228 cm^{-1} decreased while the intensities of bands at 1303, 1257 and 1183 cm^{-1} increased correspondingly during melting process

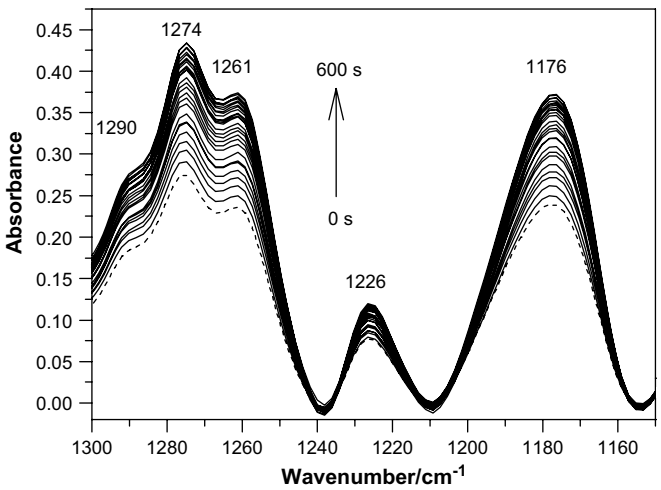

Fig. 8. FTIR spectra of the ν(C–O–C) stretching bands of PHBHHx (HHx = 12 mol%) at region of 1300–1150 cm^{-1} during water diffusion process. The short dot line represents the starting spectrum, and the spectral interval is 20 s.

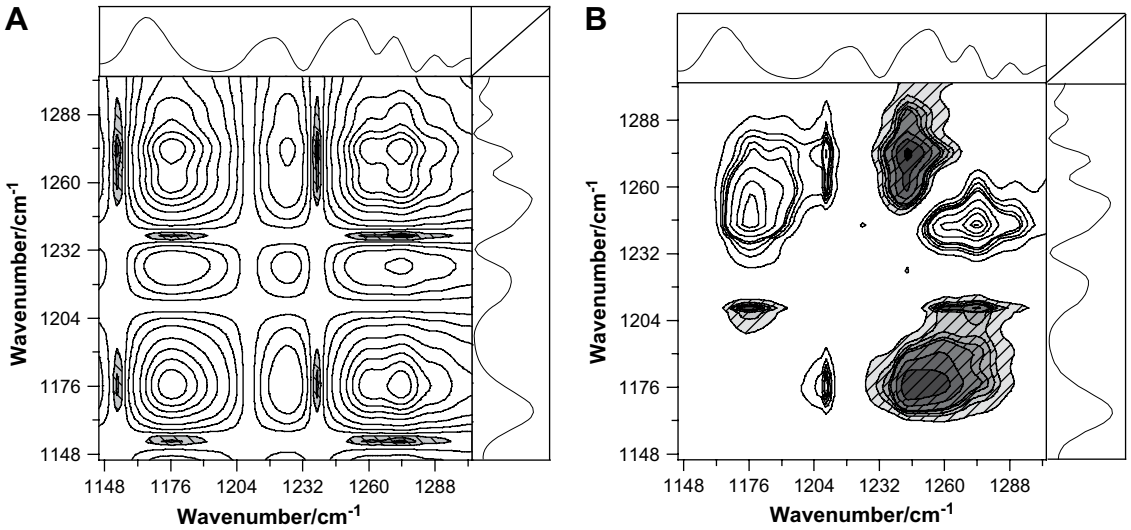

Fig. 9. Generalized 2D correlation FTIR spectra of ν(C–O–C) stretching band of PHBHHx (HHx = 12 mol%) at the region of 1300–1160 cm^{-1}. (A) and (B) are synchronous and asynchronous contour maps, respectively. The shaded and unshaded areas represent negative and positive correlation peaks, respectively.

of PHBHHx. These two groups of bands were assigned respectively to the crystalline and amorphous phases by authors. Accordingly, in our work, the changes in both crystalline phase at 1290, 1274, 1261, 1226 cm^{-1} and amorphous phase at 1176 cm^{-1} take part during the water diffusion process.

2D correlation spectroscopy in region of 1300–1160 cm^{-1} is shown in Fig. 9. The cross-peak at 1176, 1209 cm^{-1} is negative in both of the synchronous (Fig. 9A) and asynchronous spectra (Fig. 9B), and the cross-peak at 1176, 1226 cm^{-1} is positive in both of the synchronous (Fig. 9A) and asynchronous (Fig. 9B) spectra. In terms of Noda's rule [42], the change in intensity at 1176 cm^{-1} is earlier than that at 1209 cm^{-1}. Similarly, the change in intensity at 1176 cm^{-1} is earlier than that at 1226 cm^{-1}. Because the bands at 1176 cm^{-1} were assigned to the amorphous components and 1209 and 1224 cm^{-1} to the crystalline phases [20,22], the same results as previous paragraph are confirmed that firstly water molecules diffuse into the amorphous phase, and then penetrate into the crystalline phase.

3.6. Evaluation of water diffusion coefficient

Time-resolved ATR–FTIR is a powerful technique for the measurement of small molecule diffusion coefficient in the polymer because of its convenience *in situ*. It can provide reliable transient data and information at the molecular level [32]. The experimental curve was formed in terms of a series of data from the integral of ν(OH) stretching band at 3700–3000 cm^{-1} and δ(OH) bending band at 1700–1550 cm^{-1} *versus* diffusion time. The fitting result based on Eq. (2) was shown in Fig. 10, where the hollow square and solid triangle points represent experimental data, and the solid lines represent non-linear fitting curves. D_ν represents the water diffusion coefficient obtained from the fitting result of ν(OH) stretching band at 3700–3000 cm^{-1} *versus* diffusion time, equal to 8.7×10^{-8} $cm^2\,s^{-1}$ and 7.5×10^{-8} $cm^2\,s^{-1}$ obtained from two samples, respectively, shown in Fig. 10a, and D_δ represents the water diffusion coefficient obtained from the fitting result of δ(OH) bending band at 1700–1550 cm^{-1} *versus* diffusion time, equals to

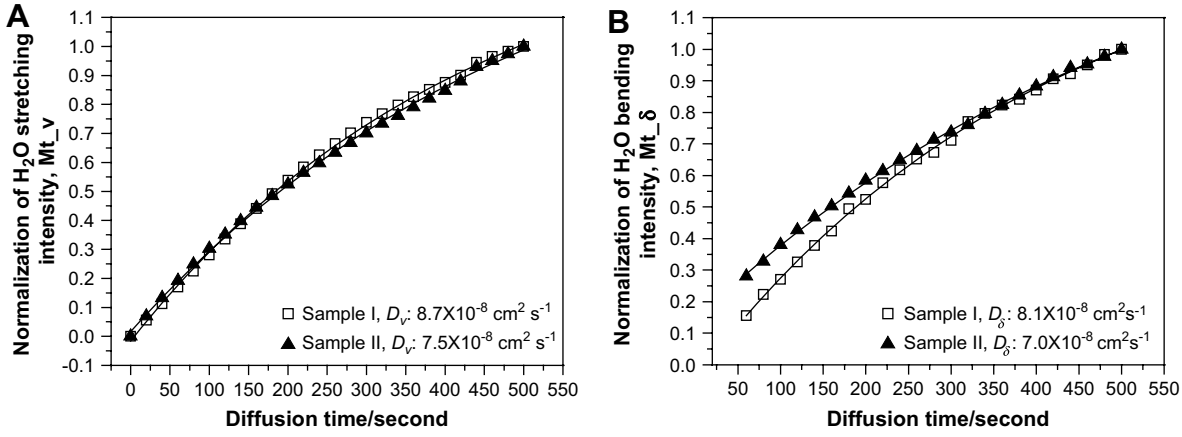

Fig. 10. Diffusion curve of water in PHBHHx matrix with crystalline degree of 16.2 ± 0.3%. The hollow square and solid triangle points represent experimental data of samples **I** and **II**, respectively, and the solid lines represent fitting curves based on Fickian model. The thickness of the polymer film $L = 97 \pm 1$ μm. (a) Represents ν(OH) stretching band at 3700–3000 cm^{-1} *versus* diffusion time; (b) represents δ(OH) stretching band at 3700–3000 cm^{-1} *versus* diffusion time. The diffusion coefficient D_ν derived from ν(OH) stretching band is 8.7×10^{-8} $cm^2\,s^{-1}$ (sample **I**, $R_\nu^2 = 0.9994$) and 7.5×10^{-8} $cm^2\,s^{-1}$ (sample **II**, $R_\nu^2 = 0.9990$) and D_δ derived from δ(OH) bending band is 8.1×10^{-8} $cm^2\,s^{-1}$ (sample **I**, $R_\delta^2 = 0.9990$) and 7.0×10^{-8} $cm^2\,s^{-1}$ (sample **II**, $R_\delta^2 = 0.9992$) at 293 K. The average water diffusion coefficient D and standard deviation of $7.8 \pm 0.7 \times 10^{-8}$ $cm^2\,s^{-1}$ was determined by two pairs of D_ν and D_δ.

8.1×10^{-8} cm^2 s^{-1} and 7.0×10^{-8} cm^2 s^{-1} obtained from two samples, respectively, shown in Fig. 10b. The average water diffusion coefficient D and standard deviation of $7.8 \pm 0.7 \times 10^{-8}$ cm^2 s^{-1} were determined by two pairs of D_ν and D_δ at temperature of 293 K. The resultant average value with error of <9% is reasonable under our experimental conditions, including sample purification, membrane preparation, ATR–FTIR measurement, etc.

Compared with the water diffusion coefficient of 1.5×10^{-8} cm^2 s^{-1} in PHB [39,41], our result of $7.8 \pm 0.7 \times 10^{-8}$ cm^2 s^{-1} in PHBHHx is larger. The fact that the PHBHHx (HHx = 12 mol%) of low crystallinity has larger water diffusion coefficient than PHB of high crystallinity was also observed in other polymers. For instance, Doppers et al. [50] investigated the water diffusion behavior in PVA-clay nanocomposites and found that the larger percentage of clay component in composite the smaller diffusion coefficient of water since the highly crystalline clay stops the water penetration through the nanocomposite. Also the water diffusion coefficients in the pure PVA were investigated by microgravimetry and found that the higher the crystalline degree of PVA membrane, the lower the values of the water diffusion coefficient [24]. Furthermore, Olkhove et al. [51] investigated water transport behaviors in PHB/PVA blends. They found that the pure PVA film showed the highest water permeability than any ratios of blend samples of between PVA and PHB.

4. Conclusions

The water diffusion process in PHBHHx film was investigated by 1D and generalized 2D correlation ATR–FTIR spectroscopy to probe the interaction between water molecules and polymer matrix. We found that there were at least three states of water, bulk water, free water and bound water, in the PHBHHx film during the process of water diffusion. Moreover, we figured out the detailed water diffusion process as: the water firstly diffuse into micro-voids of PHBHHx film in bulk water form, or is dispersed on the surface of film in free water form, and then water molecules interact with the hydrophilic groups, like C=O, C–O–C groups of PHBHHx in bound water form. Furthermore, we thought that water preferred penetrating through the loose amorphous phase to diffusing into the compact crystalline phase in PHBHHx film. According to Fickian mode [46], the water diffusion coefficient of $7.8 \pm 0.7 \times 10^{-8}$ cm^2 s^{-1} was evaluated for the PHBHHx material with crystalline degree of 16.2 ± 0.3%. The larger water diffusion coefficient of PHBHHx than that of PHB indicates that PHBHHx is more biocompatible for the tissue engineered materials, especially for the transportation process of water and the soluble nutrition into cells through polymer scaffold.

Acknowledgements

This work was supported by the National Science Foundation of China (No. 10475017 and 20673022). Authors like to thank Professor Chen G.Q. in Tsinghua University for kindly donating the PHBHHx compound.

References

[1] Zhao K, Deng Y, Chen JC, Chen GQ. Biomaterials 2003;24(6):1041–5.
[2] Chen GQ, Wu Q. Biomaterials 2005;26(33):6565–78.
[3] Doi Y, Kitamura S, Abe H. Macromolecules 1995;28(14):4822–8.
[4] Yoshie N, Menju H, Sato H, Inoue Y. Macromolecules 1995;28(19):6516–21.
[5] Sombatmankhong K, Sanchavanakit N, Pavasant P, Supaphol P. Polymer 2007;48(5):1419–27.
[6] Alata H, Aoyama T, Inoue Y. Macromolecules 2007;40(13):4546–51.
[7] Chen GQ, Zhang G, Park SJ, Lee SY. Applied Microbiology and Biotechnology 2001;57(1–2):50–5.
[8] Deng Y, Lin XS, Zheng Z, Deng JG, Chen JC, Ma H, et al. Biomaterials 2003;24(23):4273–81.
[9] Kunze C, Freier T, Kramer S, Schmitz KP. Journal of Materials Science - Materials in Medicine 2002;13(11):1051–5.
[10] Sodian R, Sperling JS, Martin DP, Egozy A, Stock U, Mayer JE, et al. Tissue Engineering 2000;6(2):183–8.
[11] Li XT, Zhang Y, Chen GQ. Biomaterials 2008;29(27):3720–8.
[12] Padermshoke A, Katsumoto Y, Sato H, Ekgasit S, Noda I, Ozaki Y. Polymer 2004;45(19):6547–54.
[13] Li Z, Tsuchiya K, Inoue Y. Macromolecular Bioscience 2004;4(8):699–705.
[14] Hu Y, Sato H, Zhang JM, Noda I, Ozaki Y. Polymer 2008;49(19):4204–10.
[15] Furukawa T, Sato H, Murakami R, Zhang JM, Noda I, Ochiai S, et al. Polymer 2006;47(9):3132–40.
[16] Cui YJ, Wang XL, Hong L, Tang XZ. Journal of Applied Polymer Science 2002;84(7):1363–8.
[17] Wong MS, Causey TB, Mantzaris N, Bennett GN, San KY. Biotechnology and Bioengineering 2008;99(4):919–28.
[18] Padermshoke A, Sato H, Katsumoto Y, Ekgasit S, Noda I, Ozaki Y. Polymer 2004;45(21):7159–65.
[19] Yoshie N, Menju H, Sato H, Inoue Y. Polymer Journal 1996;28(1):45–50.
[20] Padermshoke A, Sato H, Katsumoto Y, Ekgasit S, Noda I, Ozaki Y. Vibrational Spectroscopy 2004;36(2):241–9.
[21] Sato H, Murakami R, Padermshoke A, Hirose F, Senda K, Noda I, et al. Macromolecules 2004;37(19):7203–13.
[22] Sato H, Nakamura M, Padermshoke A, Yamaguchi H, Terauchi H, Ekgasit S, et al. Macromolecules 2004;37(10):3763–9.
[23] Qu XH, Wu Q, Liang J, Zou B, Chen GQ. Biomaterials 2006;27(15):2944–50.
[24] Perrin L, Nguyen QT, Clement R, Neel J. Polymer International 1996;39(3):251–60.
[25] Miguel O, Iruin JJ. Journal of Applied Polymer Science 1999;73(4):455–68.
[26] Sammon C, Everall N, Yarwood J. Macromolecular Symposia 1997;119:189–96.
[27] Sammon C, Yarwood J, Everall N. Polymer 2000;41(7):2521–34.
[28] Miller CE, Svendsen SA, Naes T. Applied Spectroscopy 1993;47(3):346–56.
[29] Rautenbach R, Dahm W, Herion C, Janisch I. Chemie Ingenieur Technik 1989;61(7):535–44.
[30] Deluca NW, Elabd YA. Journal of Polymer Science Part B - Polymer Physics 2006;44(16):2201–25.
[31] Miyajima M, Koshika A, Okada J, Ikeda M, Nishimura K. Journal of Controlled Release 1997;49(2–3):207–15.
[32] Elabd YA, Baschetti MG, Barbari TA. Journal of Polymer Science Part B - Polymer Physics 2003;41(22):2794–807.
[33] Tang BB, Wu PY, Siesler HW. Journal of Physical Chemistry B 2008;112(10):2880–7.
[34] deJong EAM, Kaper J. Netherlands Milk and Dairy Journal 1996;50(1):35–51.
[35] Sammon C, Deng CS, Yarwood J. Polymer 2003;44(9):2669–77.
[36] Sammon C, Mura C, Yarwood J, Everall N, Swart R, Hodge D. Journal of Physical Chemistry B 1998;102(18):3402–11.
[37] Peng Y, Wu PY, Yang YL. Journal of Chemical Physics 2003;119(15):8075–9.
[38] Peng Y, Wu PY, Siesler HW. Biomacromolecules 2003;4(4):1041–4.
[39] Iordanskii AL, Kamaev PP. Vysokomolekulyarnye Soedineniya Seriya A & Seriya B 1999;41(2):374–8.
[40] Iordanskii AL, Kamaev PP, Hanggi UJ. Journal of Applied Polymer Science 2000;76(4):475–80.
[41] Iordanskii AL, Kamaev PP, Zaikov GE. Polymer - Plastics Technology and Engineering 1999;38(4):729–38.
[42] Noda I, Dowrey AE, Marcott C. Applied Spectroscopy 1993;47(9):1317–23.
[43] Noda I. Analytical Sciences 2007;23(2):139–46.
[44] Noda I. Journal of Molecular Structure 2006;799(1–3):41–7.
[45] Zheng Z, Bei FF, Tian HL, Chen GQ. Biomaterials 2005;26(17):3537–48.
[46] Fieldson GT, Barbari TA. Polymer 1993;34(6):1146–53.
[47] Cheng S-T, Chen Z-F, Chen G-Q. Biomaterials 2008;29(31):4187–94.
[48] Zhu B, He Y, Nishida H, Yazawa K, Ishii N, Kasuya K, et al. Biomacromolecules 2008;9(4):1221–8.
[49] Shen Y, Wu PY. Journal of Physical Chemistry B 2003;107(18):4224–6.
[50] Doppers LM, Breen C, Sammon C. Vibrational Spectroscopy 2004;35(1–2):27–32.
[51] Olkhov AA, Vlasov SV, Iordanskii AL, Zaikov GE, Lobo VMM. Journal of Applied Polymer Science 2003;90(6):1471–6.
[52] Liu MJ, Wu PY, Ding YF, Chen G, Li SJ. Macromolecules 2002;35(14):5500–7.